IEEE Access
Multidisciplinary ⋮ Rapid Review ⋮ Open Access Journal

Received 8 November 2022, accepted 2 January 2023, date of publication 13 February 2023, date of current version 8 March 2023.

Digital Object Identifier 10.1109/ACCESS.2023.3244215

RESEARCH ARTICLE

Novel Integrated NLC-SHE Control Applied in Cascaded Nine-Level H-Bridge Multilevel Inverter and Its Experimental Validation

MOHD TARIQ[1,2], (Senior Member, IEEE), DEEPAK UPADHYAY[1,3], SHAHBAZ AHMAD KHAN[1], WALEED ALHOSAINI[4,5], (Member, IEEE), PASI PELTONIEMI[3], (Member, IEEE), AND ADIL SARWAR[1], (Senior Member, IEEE)

[1]Department of Electrical Engineering, Zakir Husain College of Engineering and Technology (ZHCET), Aligarh Muslim University, Aligarh 202002, India
[2]Department of Electrical and Computer Engineering, Florida International University, Miami, FL 33174, USA
[3]School of Energy Systems, Lappeenranta–Lahti University of Technology, 53850 Lappeenranta, Finland
[4]Department of Electrical Engineering, College of Engineering, Jouf University, Sakaka 72341, Saudi Arabia
[5]Engineering and Applied Sciences Research Unit, Jouf University, Sakaka 72341, Saudi Arabia

Corresponding author: Waleed Alhosaini (wsalhosaini@ju.edu.sa)

This work was supported by the Deanship of Scientific Research, Jouf University, under Grant DSR-2021-02-0396.

ABSTRACT In this paper, a novel integrated SHE-NLC control is proposed for the mitigation of unwanted lower-order harmonics in the cascaded H-bridge multilevel inverter. The proposed algorithm has been developed by hybridizing the NLC and SHE methods, in an attempt to keep the merits of both the individual control. The switching angles and nearest levels are calculated by applying the Genetic Algorithm (GA). The proposed technique reduces the calculation time and implementation complexity, thus can be a viable alternative to the real time implementation for SHE. Integrated NLC-SHE control is tested by varying the modulation index and load dynamics. This technique resulted in the reduction in Total Harmonic Distortion (THDs) in load voltage and current. Comparative analysis of NLC, SHE and Integrated NLC-SHE technique is also performed on the CHB nine-level inverter. There is significant reduction in voltage and current THD values and power losses. Efficiency of the inverter is increased. The efficacy of the proposed control CHB nine-level is tested on MATLAB Simulink environment and further validated by experimental results.

INDEX TERMS NLC, SHE, harmonic elimination, multilevel inverter, SHE, SHM, genetic algorithm, CHB.

I. INTRODUCTION

Multilevel Voltage Source Inverters (MVSIs) have emerged as the advanced and modern category of DC-AC converters or inverters used in various industrial applications including uninterruptible power supply (UPS), electric drives, renewable energy integration, active power filters etc, [1], [2]. MVSIs consists of more semiconductor devices, capacitors that are powered by DC sources. MVSIs can not only produce more voltage levels but also can operate at a high-power ratio as switches will be needed to endure lower voltage stress [3]. Neutral point clamped inverter (NPC), Flying capacitor (FC) inverter and cascaded H bridge (CHB) inverter appeared as the first generation of promising topologies for industrial applications as compared to the conventional bipolar voltage source inverters (VSIs) because of the reduction in dv/dt stress and electromagnetic interference (EMI), improved harmonic profile of the output voltage [4], [5]. Development of MVSIs led by extensive research was oriented toward novel topologies focused on increasing the voltage levels counts [6]. As the initial attempts are being inspired by the concept of CHB, the hybrid structures of traditional MVSIs such as symmetrical and asymmetrical cascaded topology were utilized for HB, NPC and FC to increase the voltage levels count and operate with higher efficiency [7], [8], [9], [10], [11]. The asymmetrically series-connected full and half-bridge has been proposed in [12] for the wide DC-link voltage variation and to double the levels of the network. In [13], [14]

The associate editor coordinating the review of this manuscript and approving it for publication was Md. Rabiul Islam.

asymmetrical cascaded H-Bridge of NPC and conventionally used two-level inverters have been presented with merits of low switching frequency operation for high voltage cell and high dynamic response.

Despite this, hybridizing the conventional MVSIs based on the symmetrical and asymmetrical cascaded connection does not optimize the MVSIs design and it significantly increases the number of components and separated DC sources and consequently manufacturing cost [15]. In [16], [17], [18], [19], [20] some innovative MVSIs have been proposed to produce a notable number of levels as similar as sinusoidal waveform without using asymmetrical and symmetrical connections. In practice, two or more H-bridge cells are cascaded together to enhance the levels in the output voltage in the cascaded H-bridge inverter [21], [22]. Thus, there is an increase in the number of switches as well as the DC power supply. The system also becomes complex. Thus, the increment is at the cost of an increase in the number of components. m-cells with as many dc power supply used in CHB-MLI can produce 2m+1 levels in the output voltage. Conversely, (N−1)/2 dc sources and (2N−1) Switches are required to generate N levels in the output voltage. The symmetric configuration of a CHB inverter needs to incorporate three DC supplies and twelve switches to generate an output voltage with seven levels. Similarly, to produce thirteen level output, the bridge needs twenty-four switches and six dc supplies. At any instant of time, twelve switches are in ON state. This increases conduction losses considerably [23]. Assuming 0.5 volts drop across each switch, 12 switches during operation cause a drop of 6 volts and consequently, the power loss is quite high under higher current operation. Thereby, efficiency reduces. A drastic reduction in switch count has been observed by the implementation of asymmetric configuration in CHB topology. Different DC supply voltage combinations in asymmetric CHB can generate various possible voltage levels [24]. When two cascaded H-bridge MLI are employed, two voltage sources and 8 switches along with a battery voltage combination ratio of 1:1 generates a five-level output voltage while 1:2 generates 7 level output voltage. A maximum possible output voltage could be generated with a voltage combination of 1:3, i.e., 9 levels. At most four switches are in ON state during any instant of operation in asymmetrical CHB-MLI [25], [26]. There is a sufficient degree of freedom and redundancy under such configuration.

Despite the many advantages of CHB Multilevel inverters, the problem of harmonics and power losses are still there. To overcome these challenges various control techniques are used to suppress these drawbacks. Several switching techniques have been proposed previously to improve the switching performance of the converters [27], [28], modulation techniques to improve the power loss division performance [29] of MLIs and modified saturated equal loading PWM [30]. In this paper a different approach has been applied by hybridizing NLC and SHE techniques to achieve the same goals of reduced THD in voltage and current waveforms and switching performance by reducing the computational complexity and time for the calculation of switching angles. Low-frequency controls like selective harmonic elimination pulse width modulation (SHEPWM), nearest level controllers (NLC), selective harmonic mitigation (SHM) are widely used techniques [31], [32], [33], [34], [35], [36], [37], [38]. In SHE, the lower order harmonics are removed by optimal switching of the inverter. This is done by solving the complex non-linear transcendental equations. The main problem associated with this control is solving these complex equations is time-consuming and cumbersome. Applying to closed-loop operation is also difficult. In the case of NLC, the switching frequency is the power frequency and also easy to implement. The major drawback backs are the first one reduction in voltage levels as the modulation index is varied and the second one is an increment in the THD values in load voltage and current. To incorporate the advantages of both NLC and SHE a new control is proposed in this paper. The optimal switching angles for the wide range of modulation index using genetic algorithm [39], [40] has been found and then corresponding nearest level rounding of values are calculated to apply these values in NLC. The equations now relate the nearest level values to the modulation index linearly and also keeping the benefits of SHE. In this paper, to generate 9 levels output voltage waveform, CHB-MLI with asymmetrical structure, employing two voltage sources and eight IGBT switches has been used. A novel control strategy, formed by hybridizing NLC and SHE is used to control the output voltage. This hybrid control can enhance the controllability of the output voltage at minimum THD. This hybrid control scheme has been applied to CHB-MLI and thorough analysis has been performed under varying loading and dynamic conditions. This technique has been simulated in MATLAB/Simulink environment. This hybridized controlling technique has been simulated in a MATLAB/Simulation environment. The scheme has also been simulated for thermal modelling on PLECS software and power loss analysis has been performed. The prototype of the cascaded H- bridge inverter has also been developed and the proposed control scheme has been implemented.

This paper has been organized as follows: introduction of cascaded H-Bridge inverter and NLC and SHE is discussed in section II. Section III discusses the proposed integrated nearest level controller. Section IV provided the simulation result analysis and comparative study for the proposed integrated NLC-SHE control, NLC, SHE techniques, considering various circuit parameters. Hardware results have been presented in section V which is validated by experiment on a prototype of the MLI. The conclusion is presented at the end.

II. CASCADED H-BRIDGE NINE LEVEL INVERTER

Cascaded H-bridge MLI is simple, reliable having a modular structure. There is no need for clamping diodes in CHB. As compared to other topologies these features make CHB more preferable [41], [42], [43]. CHB- MLI can have both symmetrical or asymmetrical structure. In symmetrical CHB-MLI, the equal value of the DC sources is employed.

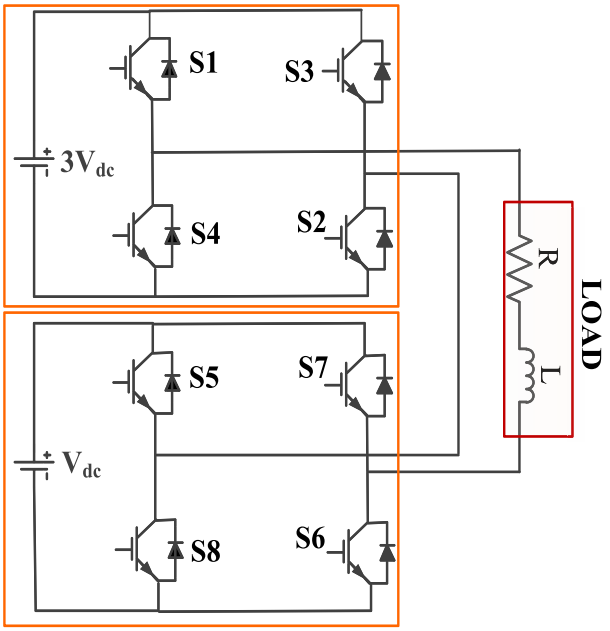

FIGURE 1. Circuit diagram of CHB nine level inverter.

However, in asymmetrical CHB-MLI, DC sources of unequal magnitude are employed [44]. In the case of asymmetrical MLI, more levels can be produced as compared to symmetrical MLI, employing the same number of DC voltage supply and switches. Each full-bridge or H-Bridge cell is capable of generating three levels (−Vdc, +Vdc, 0). 'N' number of voltage levels can be generated using the 'K' number of DC sources where $N = 2K + 1$.

A. NEAREST LEVEL CONTROL (NLC)

Multilevel inverter operation can be categorized based on the modulation strategies as (1) fundamental and (2) high switching frequency modulation. As the operation of MLIs at higher switching frequency leads to considerable switching losses in the inverter. Thus, in high power applications fundamental or low switching frequency (<1KHz) modulation scheme is preferred in order to avoid the appreciable losses. The nearest level control works at the fundamental frequency. This scheme is efficient and fast in terms of implementation procedures. Nearest Level Control (NLC) operates at 50Hz or 60Hz and can easily be extended to N levels. It is a conventional method of control which simply rounds (Y) by taking the half integer value as the comparing value where $F_{round}(Y)$ is the integer close to reference value. A smaller step size can be used to improve the performance.

For the generation of gating signal to operate, it is then passed through the switching algorithm. The calculation time and expense can be reduced by the implementation of digital logic gate, which ultimately simplifies the switching state. The major demerit of this control is that the harmonics in the output voltage. The harmonics in the output voltage is high for lower modulation index and lesser no. of levels. The

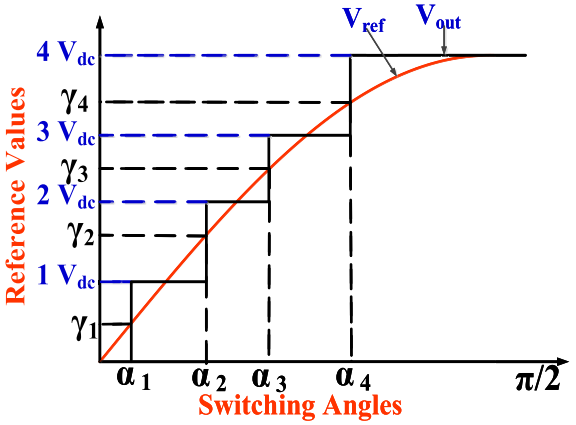

FIGURE 2. Interrelating of NLC and SHE.

expression for the output voltage wave is

$$V_{out} = M_a \times \frac{N-1}{2} \times V_{dc} \times \cos(\omega t) \tag{1}$$

where M_a is the modulation index and N is the number of output levels. Fig. 2 shows the conventional nearest level control scheme. For optimization purposes, a constant carrier value can be determined for the conventional NLC method. By the comparison of reference signal with the distinct nearest level and switching angle variation, the optimal value of the constant carrier can be found out. This is called as Optimum NLC (ONLC). Thus, ONLC, which has been applied in this paper, has emerged as an ideal scheme to generate staircase output voltage waveform with low THD and high RMS value. The value of M_n which gives lowest harmonics with the increased RMS voltage is chosen as optimum value.

B. SELECTIVE HARMONIC ELIMINATION (SHE)

SHEPWM technique is used for [31], [32] multilevel inverters for removing the lower order harmonics. Also, the switching frequency is lower which makes it suitable for high power converters. Filter size is also reduced. The major disadvantage related to the SHE is solving of transcendental equations every time as the modulation index is changed. Calculation of switching angles every time is time consuming and cumbersome. In this paper, the lower order harmonics that is 3rd, 5th and 7th are targeted and removed. The calculation of switching angles is done by metaheuristic based iterative method that is genetic algorithm. GA is used for local filtering of minima around the best solution. The general flourier series expansion for nine level inverter for minimizing the lower order harmonics is given by

$$V(\omega t) = \sum_{n=1}^{\infty} (V_n) \sin(n\omega t) \tag{2}$$

where V_n is the nth harmonic amplitude and now calculate using equation (3)

$$V_n = \begin{cases} \frac{4V_{dc}}{n\pi} \sum_{n=1}^{\infty} (k_i) \sin(n\omega t) & \textit{for odd n values} \\ 0 & \textit{for even n values}. \end{cases} \tag{3}$$

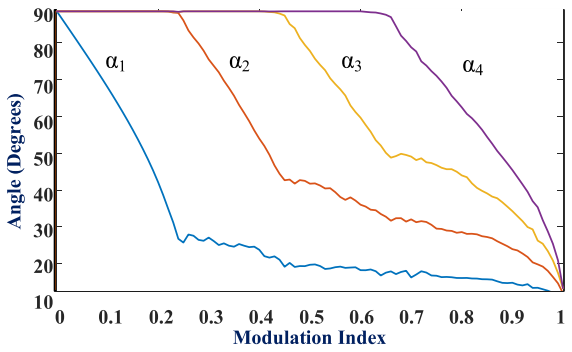

FIGURE 3. Simulation result of Nine-level switching angles loci for 9-level inverter over the whole range of modulation index.

where V_{dc} is the nominal DC voltage and ($n\omega t = n\theta$) are the firingangles calculated in the order $\left(0 < \omega t_1 \ldots < \omega t_s \leq \frac{\pi}{2}\right)$. k_i is the ratio of V_{dci} to V_{dc}. In this paper, 3rd, 5th & 7th harmonics in the 9-level are considered to eliminate from MLI. The primary role of SHEPWM method is to obtain the switching angles that regulate the fundamental at the desired level $V_{desired}$ with the additional benefit of removing the unwanted lower-order harmonics for the MIs which has solutions. The optimized firing angles for the 9-level inverter having equal DC sources ($k_1 = k_2 = k_3 = k_4 = 1$) are obtained using equation (3).

$$M_a = 1/3[cos(\theta_1) + cos(\theta_2) + cos(\theta_3) + cos(\theta_4)] \quad (4)$$
$$[cos3(\theta_1) + cos3(\theta_2) + cos3(\theta_3) + cos3(\theta_4)] = 0 \quad (5)$$
$$[cos(5\theta_1) + cos(5\theta_2) + cos(5\theta_3) + cos5(\theta_4)] = 0 \quad (6)$$
$$[cos(7\theta_1) + cos(7\theta_2) + cos(7\theta_3) + cos7(\theta_4)] = 0 \quad (7)$$

III. PROPOSED INTEGRATED NLC-SHE CONTROL

In this proposed control the benefits of both NLC and SHE techniques are integrated together. This is done by finding optimum, triggering angles using GA as shown in Fig. 3, and then calculating the corresponding nearest values for NLC. At these values, the desired harmonics are removed. Initially, the transcendental equations (4) and (5) are solved for finding optimal angles for removing the desired harmonics for modulation index range of (0 to 1). Further, nearest levels corresponding to these values are calculated and new polynomial equations relating the modulation index with nearest values are found. Mathematically the integration of these two (NLC & SHE) controls is validated by using the equations (1) to (7).

The general equation for NLC is given in equation (8) in which V_{dc} is given by:

$$V_{dc} = M_a \times V_{dc} Sin\alpha \quad (8)$$

Here α is the triggering angle in case of NLC. If the modulation of NLC is considered the new equation is:

$$m_n \times V_{dc} = M \times V_{dc} Sin\alpha \times m_n = M * Sin\alpha \quad (8.1)$$
$$\alpha = sin^{-1}\frac{m_n}{n} \quad where, M = \left(\frac{N-1}{2}\right) \quad (8.2)$$

Here the value of N=9, as NLC is being applied on 9-level inverter. Therefore, M = 4, where N is the number of output voltage levels.

$$\alpha_{i+1} = sin^{-1}\left(\frac{m_n + i}{\frac{(N-1)}{2}}\right) \quad (9)$$

where I = 0, 1, 2, ...((N − 1)/2), m_n is the modulation index for NLC, 0 < mn < 1. Different values of α can be evaluated using equation (9) and for 9-level CHB N=9,

$$\alpha_1 = sin^{-1}\left(sin^{-1}\left(\frac{m_n}{4}\right)\right) \quad (10)$$
$$\alpha_2 = sin^{-1}\left(sin^{-1}\left(\frac{m_{n+1}}{4}\right)\right) \quad (11)$$
$$\alpha_3 = sin^{-1}\left(sin^{-1}\left(\frac{m_{n+2}}{4}\right)\right) \quad (12)$$
$$\alpha_4 = sin^{-1}\left(sin^{-1}\left(\frac{m_{n+3}}{4}\right)\right) \quad (13)$$

Using above equations (10-13), values of α_1, α_2, α_3 and α_4 can be calculated for different value of modulation index M_a. Now these values of triggering angles are put into the equations (4 and 5) of SHE where the θ is replaced by α.

$$\begin{aligned} m_a = 1/3[&cos(sin^{-1}\left(sin^{-1}\left(\frac{m_n}{4}\right)\right)) \\ &+ cos(sin^{-1}\left(sin^{-1}\left(\frac{m_{n+1}}{4}\right)\right)) \\ &+ cos(sin^{-1}\left(sin^{-1}\left(\frac{m_{n+2}}{4}\right)\right)) \\ &+ cos(sin^{-1}\left(sin^{-1}\left(\frac{m_{n+3}}{4}\right)\right))] \end{aligned} \quad (14)$$

$$\begin{aligned} [&cos3(sin^{-1}\left(sin^{-1}\left(\frac{m_n}{4}\right)\right)) \\ &+ cos3(sin^{-1}\left(sin^{-1}\left(\frac{m_{n+1}}{4}\right)\right)) \\ &+ cos3(sin^{-1}\left(sin^{-1}\left(\frac{m_{n+2}}{4}\right)\right)) \\ &+ cos3(sin^{-1}\left(sin^{-1}\left(\frac{m_{n+3}}{4}\right)\right))] = 0 \end{aligned} \quad (15)$$

$$\begin{aligned} [&cos(5sin^{-1}\left(sin^{-1}\left(\frac{m_n}{4}\right)\right)) \\ &+ cos(5sin^{-1}\left(sin^{-1}\left(\frac{m_{n+1}}{4}\right)\right)) \\ &+ cos(5sin^{-1}\left(sin^{-1}\left(\frac{m_{n+2}}{4}\right)\right)) \\ &+ cos5(sin^{-1}\left(sin^{-1}\left(\frac{m_{n+3}}{4}\right)\right))] = 0 \end{aligned} \quad (16)$$

$$\begin{aligned} [&cos(7sin^{-1}\left(sin^{-1}\left(\frac{m_n}{4}\right)\right)) \\ &+ cos(7sin^{-1}\left(sin^{-1}\left(\frac{m_{n+1}}{4}\right)\right)) \\ &+ cos(7sin^{-1}\left(sin^{-1}\left(\frac{m_{n+2}}{4}\right)\right)) \\ &+ cos7(sin^{-1}\left(sin^{-1}\left(\frac{m_{n+3}}{4}\right)\right))] = 0 \end{aligned} \quad (17)$$

The equations relating stepped nearest level values (γ_n) with the triggering angles determined from selective harmonic elimination (SHE) can be related

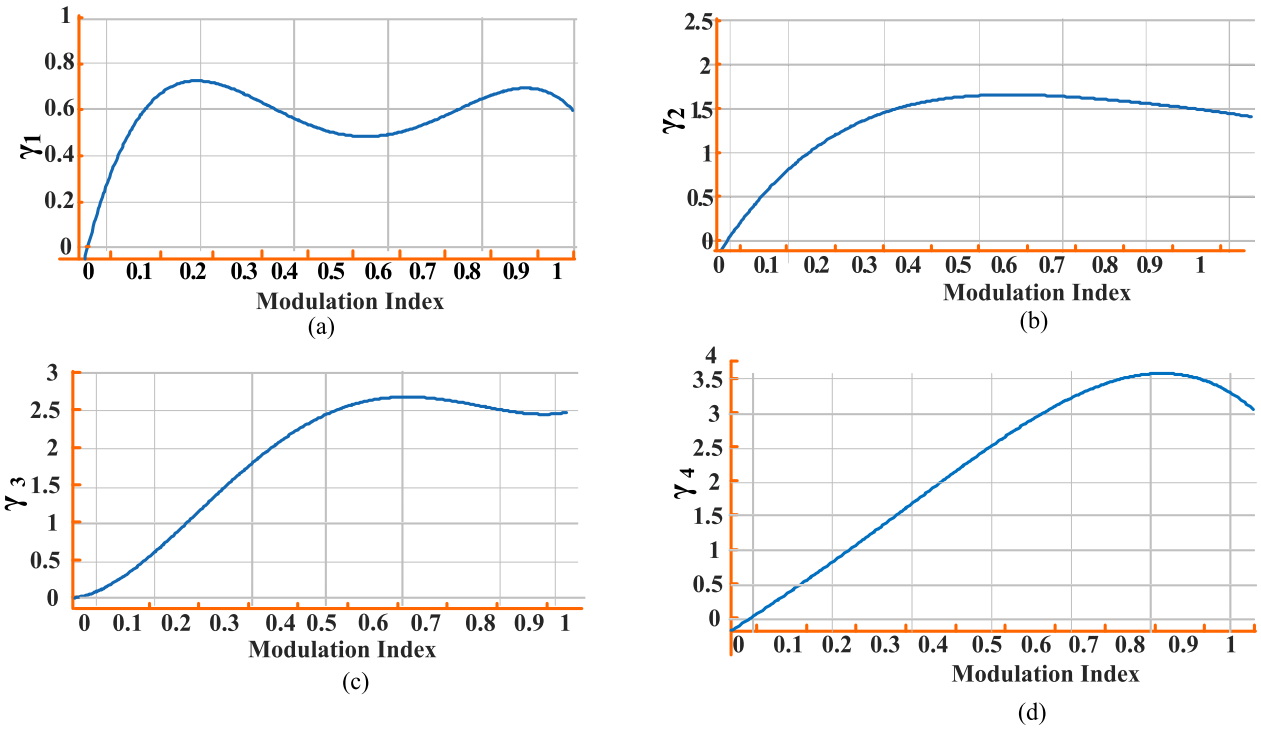

FIGURE 4. Simulation results of Nearest Level values varying with modulation index.

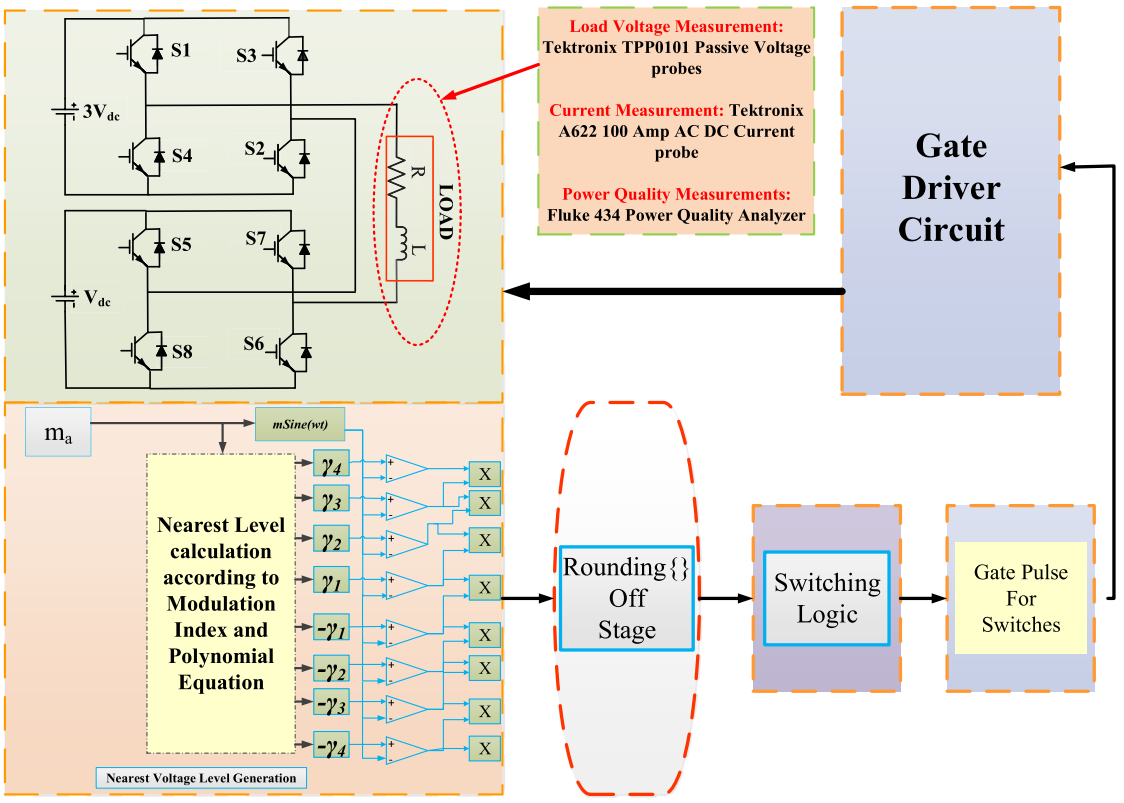

FIGURE 5. Block diagram of implementation of integrated NLC-SHE control and its Power Circuit.

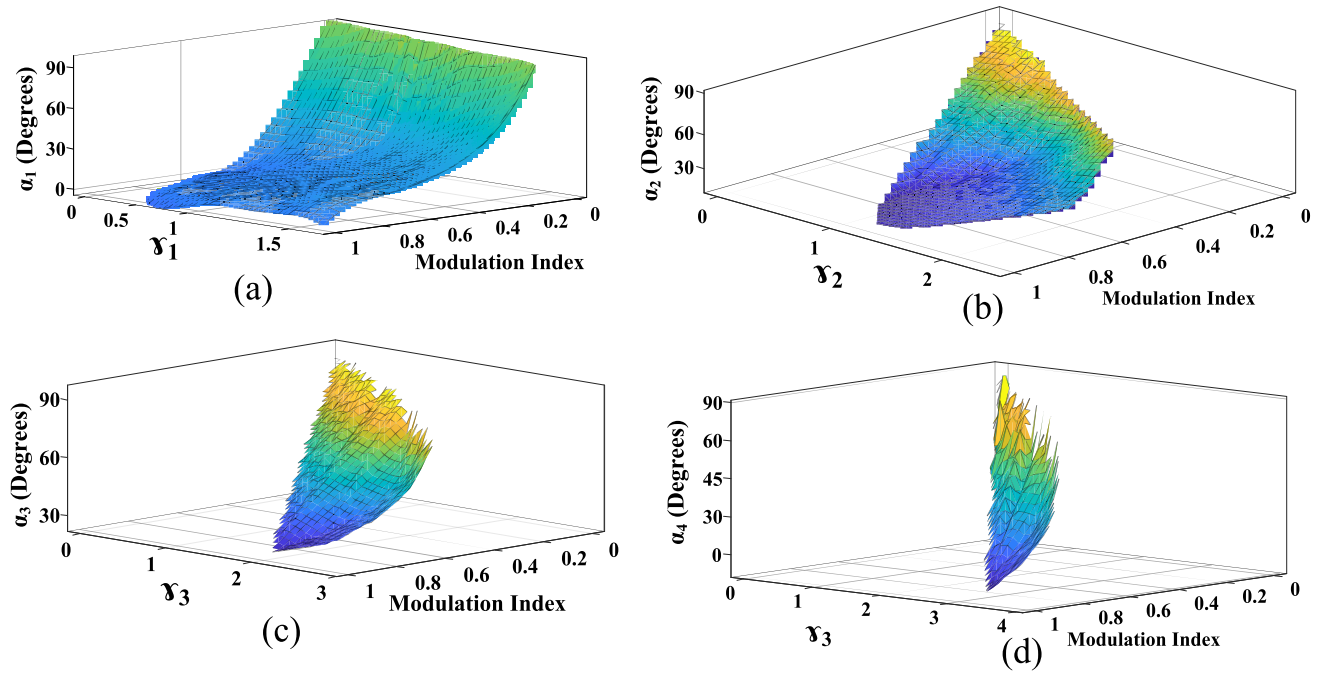

FIGURE 6. Simulation results of 3D plane diagram showing relation between modulation index, SHE triggering angles (α_s), NLC (γ_n) values.

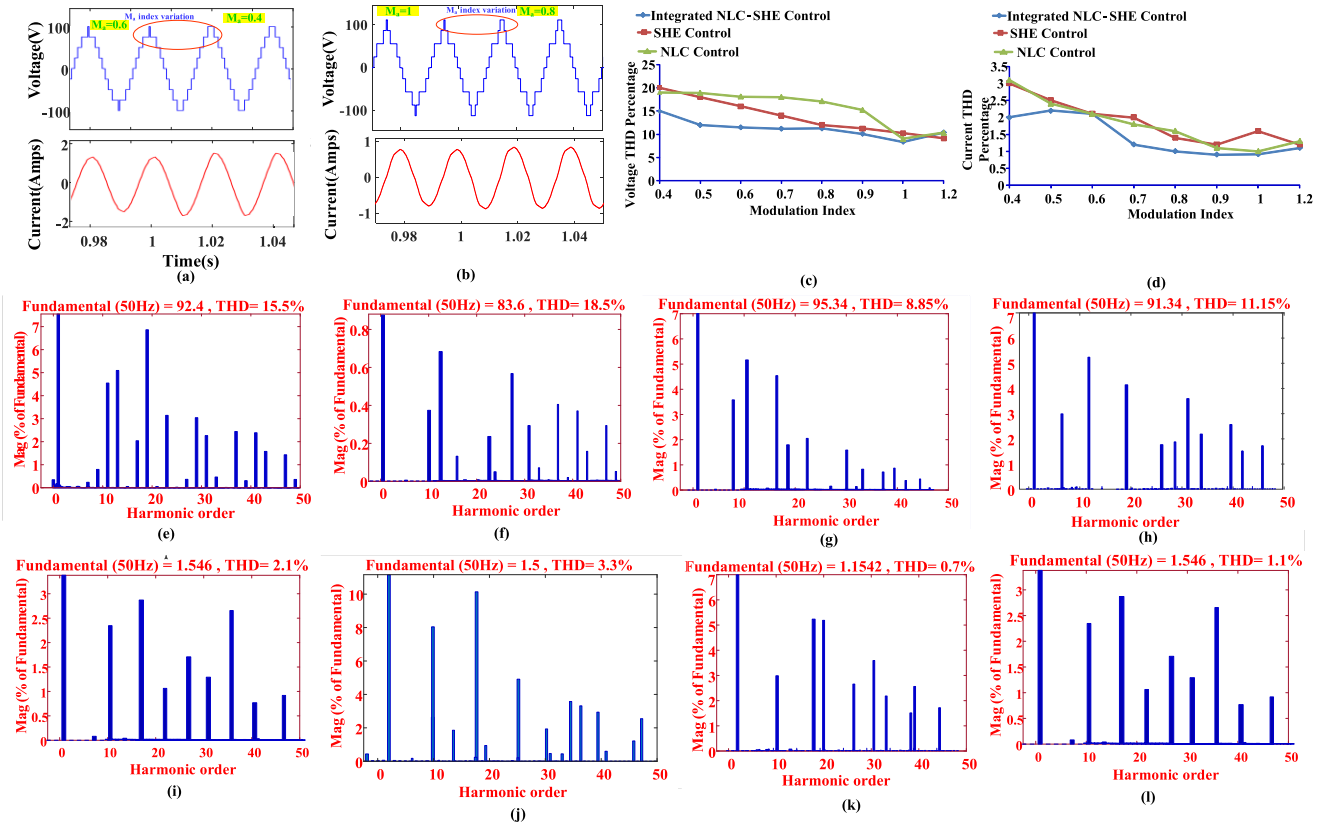

FIGURE 7. Simulation results of (a) change of MI (0.6 to 0.4) with RL load (b) change of MI (1 to 0.8) with RL load (c) Voltage THD variation with modulation index for SHE, NLC, integrated NLC-SHE Control. (d) Current THD variation with modulation index for SHE, NLC, Integrated NLC-SHE Control.(e) voltage FFT (MI=0.6, R load) (f) voltage FFT (MI=0.4, R load) (g) voltage FFT (MI=1, R load) (h) voltage FFT (MI=0.8, R load) (i) current FFT (MI=0.6, R load) (j) current FFT (MI=0.4, R load) (k) current FFT (MI=1, R load) (l) current FFT (MI=0.8, R load).

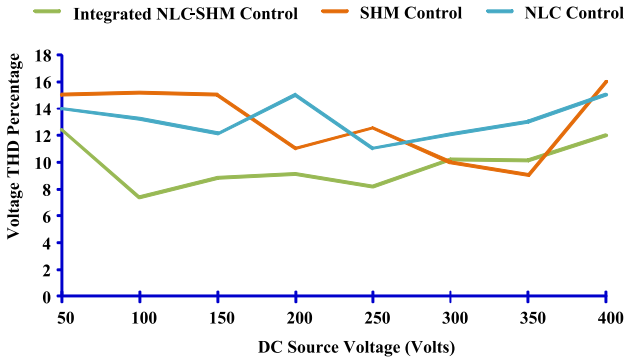

FIGURE 8. Simulation results of variation of load voltage THD percentage with DC source voltage.

from the following equations:

$$\gamma_n = (\frac{N-1}{2}) \times m_a \times sin\,(\alpha_n) \tag{18}$$

As N = 9 and $0 < m_a < 1$,

$$\gamma_1 = 4 \times m_a \times sin\,(\alpha_1) \tag{19}$$
$$\gamma_2 = 4 \times m_a \times sin\,(\alpha_2) \tag{20}$$
$$\gamma_3 = 4 \times m_a \times sin\,(\alpha_3) \tag{21}$$
$$\gamma_4 = 4 \times m_a \times \sin\,(\alpha_4) \tag{22}$$

Solving these equations from (14) to (22), We get a polynomial function relating the modulation index to the nearest values of NLC. This function is used in control block to generate the γ_n values for various modulation index variations.

$$f(x) = p_1 \times x^4 + p_2 \times x^3 + p_3 \times x^2 + p_4 \times x + p_5 \tag{23}$$

The value of $p1$, $p2$, $p3$ *and* $p4$ is different for different γ. The set of values for p1, p2, p3 and p4 corresponding to different γ are shown in Table 1. Fig. 4 shows variation of the F_{round} values γ_n which is the round off value close to integer value) with the modulation index (M_a). For γ_1, its value first increases with modulation index (M_a) then there is a dip and it again increase with the increasing modulation index. The value of γ_2, first increases with the increasing modulation index upto ma=0.5 and then there is slight decrease and it almost settle at $\gamma_2 = 1.5$. For the other two values of γ (that is γ_3 and γ_4), initially their values increases steadily with the increasing modulation index (m_a) and then show a slight dip at the value of m_a close to unity. Fig. 4 shows the control strategy for integrated NLC-SHE control. The modulation index values are fed to nearest value controller which using the polynomial function generates the γ_n values which are then compared with the sinusoidal reference signal. In the next stage these values are then controlled and the output is rounded off to nearest values. Positive four levels are generated by this and the negative four levels are generated in the same way taking the $-\gamma_n$ values. Switching logic is applied according to the state table.

TABLE 1. Coefficients of polynomial equation for various NLC values.

NLC values	*p1*	*p2*	*p3*	*p4*	*p5*
γ_1	-3.314	11.23	-14.82	8.415	-0.1336
γ_2	13.13	-28.47	15.16	2.531	0.07984
γ_3	-14.29	34.16	-27.04	7.872	-0.04477
γ_4	-3.796	1.506	0.9481	4.613	0.02025

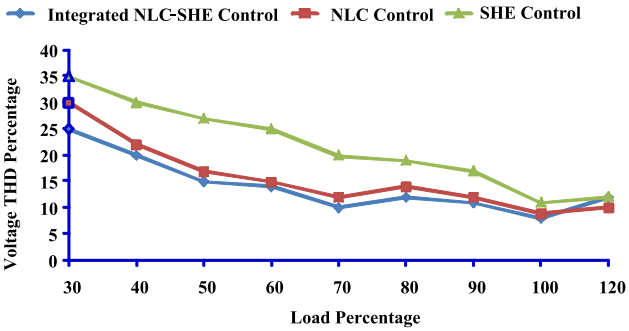

FIGURE 9. Simulation results of variation of voltage THD percentage with load percentage.

IV. SIMULATION RESULTS AND ANALYSIS

The proposed control is tested on CHB nine level inverter using MATLAB Simulink Environment. The source DC voltage taken was 100V and switching frequency taken were the power frequency of 50Hz.The topology is simulated for varying modulation index and THD profile is observed. Integration of NLC and SHE is verified by the 3D graphs shown in the Fig. 6. In the figure it is seen that the variation of γ_1 and α_1 with modulation index have widely distributed values. The relationship is approximately linear as seen in Fig. 6(a). For γ_2 and α_2, the variation in α_2 is linear but α_2 is non-linearly varied for lower modulation index values and nearly linear around unity modulation index as shown in Fig. 6(b). The variation in γ_3, γ_4 and α_3, α_4 is almost same just the variation in γ is more as depicted in Fig. 6(c) and Fig. 6(d).

Fig. 7(a) shows the load voltage and current when Modulation index varies from 0.6 to 0.4 for R-L load of 50Ω and 20mH. The voltage waveform have nine levels in the output at lower modulation index and lower order harmonics are also mitigated. Fig. 7(b) shows the load voltage and current, when Modulation index varies from 1 to 0.8 for R-L load of 50Ω and 20mH. It clearly shows that the load voltage at all modulation index values has nine levels and peak voltage is constant at 100V. Fig. 7(c) and (d) shows the change in the percentage THD in the voltage and current with the varying modulation index (Ma), when the three different control techniques namely NLC, SHE and Integrated NLC-SHE control have been applied on nine level CHB-MLI. It can be noticed from the Fig. 7(c) that the percentage THD in the voltage decreases with the increase in the modulation index (Ma), the percentage THD is not monotonous but varies in a zig-zag manner that when the Ma is increased from 0.3 to 0.4 it decreases slightly and for 0.5<Ma<0.8, the percentage

TABLE 2. Hardware parameters for experimental validation.

SNo.	Parameter	Experimental Value	Quantity
1.	DC Source Voltage	100V	1
2.	Peak to Peak Voltage	100V	-
3.	Frequency	50Hz	-
4.	Switching Frequency	50Hz	-
5.	Capacitors	4700μF,50V	2
6.	Resistive Load	30Ω,60Ω,120Ω	2
7.	Inductive Load	40mH	1
8.	Controller	TMS320F2837 D	1

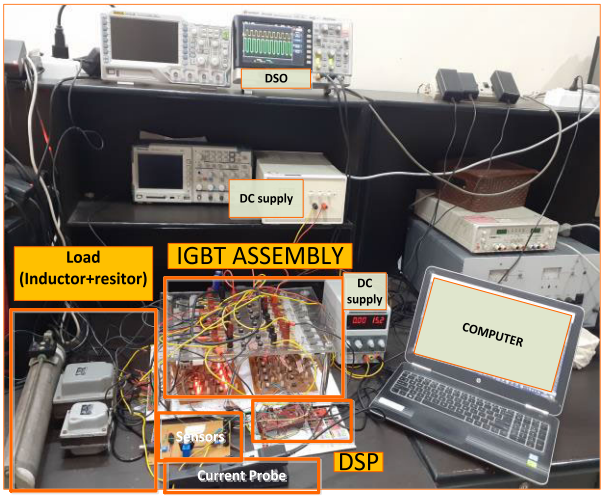

FIGURE 10. Hardware setup for experimental validation.

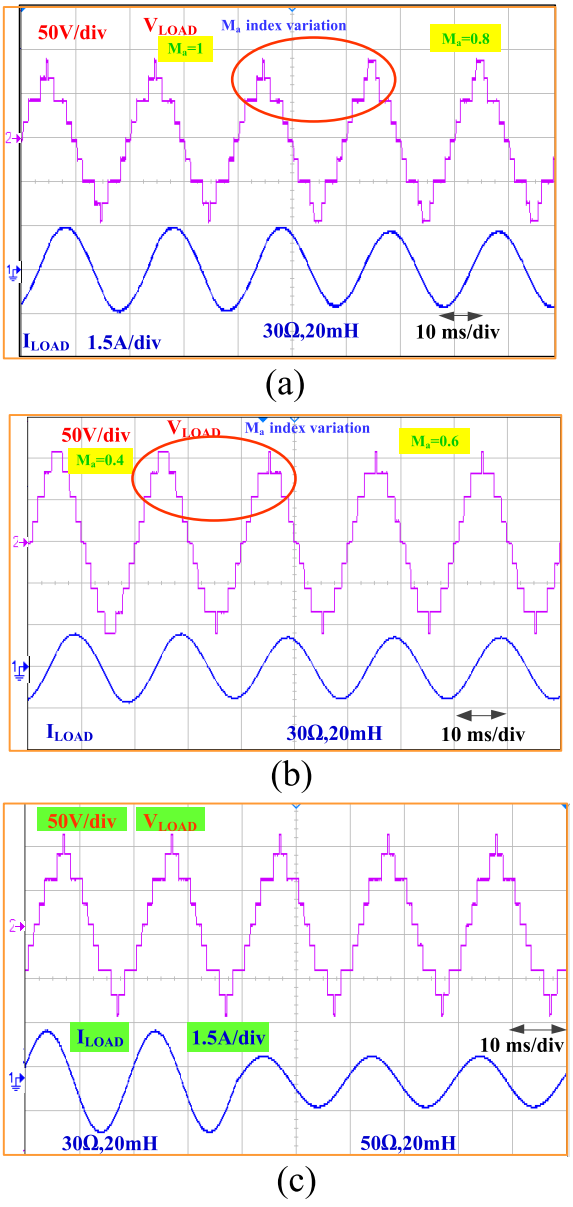

FIGURE 11. Experimental Output voltage and current waveforms (a) (a) change of MI (0.6 to 0.4) with RL load (b) change of MI (1 to 0.8) with RL load (c) for variable load.

voltage THD increases and again starts decreasing till Ma becomes unity and when operated under over-modulation range (1<Ma<1.2), it again starts increasing and reach a value of around 12%. Percentage THD voltage variation for SHE control firstly, sharply decrease till Ma=0.8 and then start decrease with relatively low gradient. Corresponding to NLC control, it first decrease slowly till Ma=0.8, then sharply decreases till Ma=1 and then again increases in the over-modulation region. In Fig. 7(d), the percentage THD in the output current remains lowest for the whole range of M_a variation. On the other hand, percentage THD in the current remains almost same for individual NLC and SHE control.

Fig. 8, shows the variation in the percentage THD in the voltage with the change in the DC source voltage. It can be noticed that for the range of DC source voltage from 50V to 300V, the percentage THD voltage corresponding to integrated NLC-SHE control found to be least, compared to other two controls (NLC and SHE), whereas as the DC source voltage is increased above 300V, Percentage voltage THD becomes comparable with that corresponding to SHE control. For a range of the DC source voltage variation from 50V to around 170V, percentage THD in the load voltage corresponding to NLC is lesser compared to SHE and when DC source voltage is increased above this value, Percentage THD becomes comparable. In Fig. 9, the variation in the percentage THD in the load voltage with the load percentage has been depicted, when the three different controls (integrated NLC-SHE, NLC and SHE) have been applied. It can be noticed that the percentage THD in the voltage variation is least for integrate NLC-SHE control followed by individual NLC and SHE for a wide variation in the load percentage (30% to 120%).

V. EXPERIMENTAL RESULTS

A 200V-600W experimental prototype has been designed to check the operability and confirming the simulation results

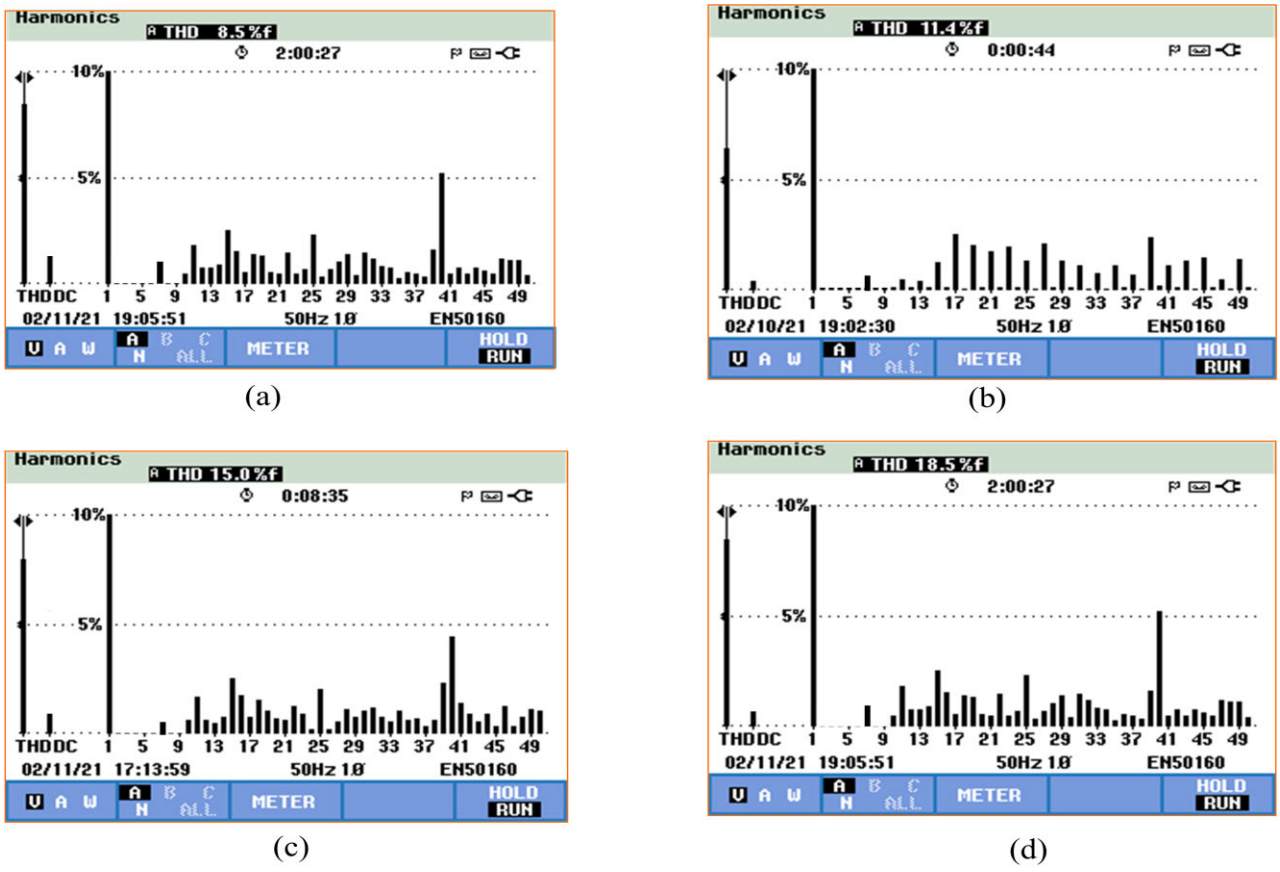

FIGURE 12. Hardware Voltage THD spectrums for (a) MI=1 (b) MI=0.8 (c) MI=0.6 (d) MI=0.4.

for validating the simulation results obtained by applying the proposed integrated NLC-SHE control. The dynamic behavior of the load and modulation index is tested on hardware prototype. The output frequency and switching frequencies selected are same that is 50Hz. The maximum input voltage is 100 Volts. Experimental setup has been shown in Fig. 10. The gate pulses are generated by Texas DSP TMS320F28379D and the dead time was taken as 5 microseconds. The Fig. 11, (a) and (b) depicts the results obtained after hardware implementation of the CHB Inverter with the proposed integrated NLC-SHE control. Fig. 11(a) and (b) shows the effects of the applied control on the load voltage and current THD waveforms with a wide variation in the modulation index (Ma). In Fig. 11(a), the modulation index is varied from 1 to 0.8 and in Fig. 10(b), Ma is varied from 0.4 to 0.6. In Fig. 11, As there is a drawback of NLC that at lower value of Ma, the number of levels decreases considerably and voltage waveshape distorts, but it can be noticed from the Fig. 11(a) and (b) shows that with the application of the proposed control, the number of voltage levels as well as the voltage magnitude remains unchanged. In Fig. 11(c), the changes in the voltage wave shape, number of levels and current waveshape with the change in the load impedance is depicted. The load impedance is varied from (30Ω, 20mH) to (50Ω, 20mH) and it can be noticed that unlike conventional NLC, the change voltage waveshape with load variation is negligible and the number of levels in the voltage waveform remains same and the load current changed accordingly. Voltage harmonic spectrums for different modulation indices are shown in Fig. 12 and is measured using Fluke 434 Power Quality Analyzer. It is seen that the lower order harmonics are mitigated from the load voltage output for the whole range of modulation index. The following hardware results are found to be consistent with the simulation results with the proposed integrated NLC-SHE control and confirms its satisfactory operation.

Power loss analysis has been performed by PLECS Simulation software and also verified on actual hardware. Loss breakup is shown in Fig. 13(a). Comparative analysis of losses in NLC, SHE, Integrated NLC-SHE is performed. Fig. 13(a) clearly shows the switching and conduction losses in employing all the three control techniques. In Fig. 13(b), shows the variation in the percentage efficiency with the varying output power (0-600W), when the three different control techniques namely NLC, SHE and integrated NLC-SHE control have been applied. It can be noticed that although the percentage efficiency values are close for all the controls, but for most of the values of output power, the percentage efficiency is lowest for SHE and in the range of 100-350W, the percentage efficiency is highest for integrated NLC-SHM

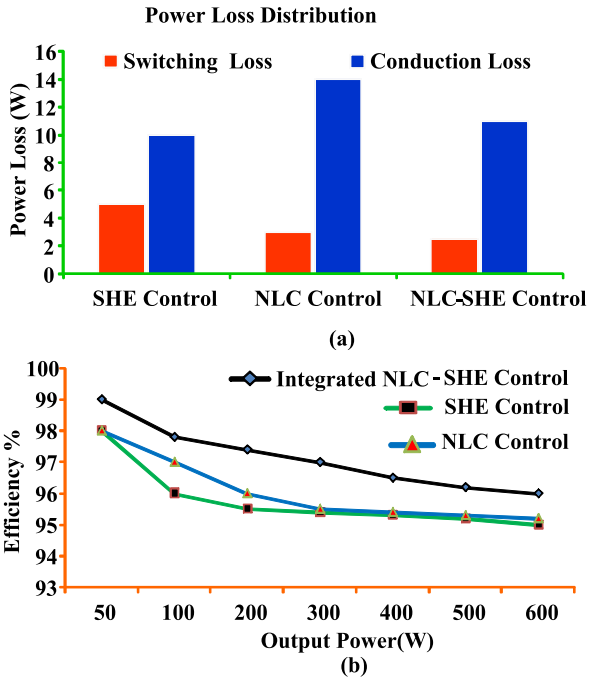

FIGURE 13. Comparison of controls on the basis of (a) Power loss distribution (b) Efficiency.

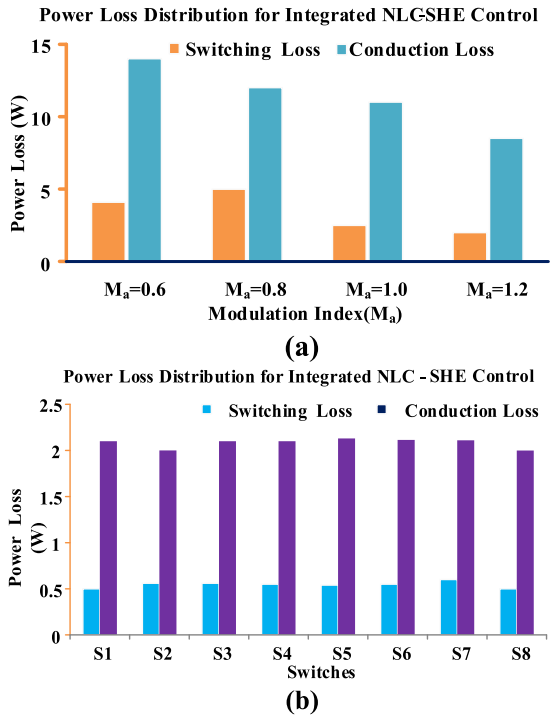

FIGURE 14. Power loss distribution for (a) varying modulation index for proposed control (b) across each switch.

control. Fig. 14(a) shows the power loss distribution of the inverter under the varying modulation index (M_a). From the bar graph, it can be easily observed that as the modulation index is increased from $M_a = 0.6$ to $M_a = 0.8$, switching losses increase slightly whereas the conduction losses are decreased. At $M_a = 1.0$, there is considerable decrease in the switching losses as it get decreased from 5W to approximately 2.5W. When the modulation index is increased further above unity (ie over-modulation operation), it was observed that the inverter with hybrid NLC-SHE control exhibit even better performance in terms of power losses (as both switching and conduction losses are lesser compared to lower modulation index range). It can be seen from Fig. 14(b) that when NLC-SHE control has been applied on CHB inverter, the power losses across each individual switch is approximately equal as the voltage stress is also evenly distributed. Proposed technique resulted in lesser losses and higher efficiencies over the wide range of rated power.

VI. CONCLUSION

This paper proposes novel integrated NLC-SHE control. It incorporated all the benefits of SHE and NLC. Non-linear transcendental equations are changed to linear polynomial equations reducing the complexity and calculation time. The efficacy of the proposed control is tested by simulation and validated experimentally. The THD percentage in load volatge and current is lesser in case of Integrated NLC-SHE, compared to conventional NLC and SHE control. The simulation results also proved that the targeted 3^{rd}, 5^{th} and 7^{th} harmonics have been reduced and the total voltage levels in output remain nine for wide range of modulation index. The prosed control is compared and found to be superior than the traditional NLC and SHE control. Power loss analysis was done using the PLECS software and losses were found to be minimum when the proposed control based triggering pulses were applied. Efficiency of the inverter also improved by applying the proposed control. Experimental results validated the simulation results and verified the operation of inverter under dynamic loading and changing modulation index. Future work could be extension of selective harmonic mitigation techniques with NLC which will target all the harmonics upto 49^{th} order.

REFERENCES

[1] J. Chavarria, D. Biel, F. Guinjoan, C. Meza, and J. J. Negroni, "Energy-balance control of PV cascaded multilevel grid-connected inverters under level-shifted and phase-shifted PWMs," *IEEE Trans. Ind. Electron.*, vol. 60, no. 1, pp. 98–111, Jan. 2013.

[2] G. Buticchi, E. Lorenzani, and G. Franceschini, "A five-level single-phase grid-connected converter for renewable distributed systems," *IEEE Trans. Ind. Electron.*, vol. 60, no. 3, pp. 906–918, Mar. 2013.

[3] L. G. Franquelo, J. Rodriguez, J. I. Leon, S. Kouro, R. Portillo, and M. A. M. Prats, "The age of multilevel converters arrives," *IEEE Ind. Electron. Mag.*, vol. 2, no. 2, pp. 28–39, Jun. 2008.

[4] H. Peng, Z. Yuan, X. Zhao, B. Narayanasamy, A. Deshpande, A. I. Emon, F. Luo, and C. Chen, "Improved space vector modulation for neutral-point balancing control in hybrid-switch-based T-type neutral-point-clamped inverters with loss and common-mode voltage reduction," *CPSS Trans. Power Electron. Appl.*, vol. 4, no. 4, pp. 328–338, Dec. 2019, doi: 10.24295/CPSSTPEA.2019.00031.

[5] X. Guo, Y. Bai, and B. Wang, "A programmable single-phase multilevel current source inverter," *IEEE Access*, vol. 7, pp. 102417–102426, 2019, doi: 10.1109/ACCESS.2019.2931741.

[6] Y. M. Ye, K. W. E. Cheng, J. F. Liu, and K. Ding, "A step-up switched-capacitor multilevel inverter with self-voltage balancing," *IEEE Trans. Ind. Electron.*, vol. 61, no. 12, pp. 6672–6680, Dec. 2014.

[7] R. Castillo, B. Diong, and P. Biggers, "Single-phase hybrid cascaded H-bridge and diode-clamped multilevel inverter with capacitor voltage balancing," *IET Power Electron.*, vol. 11, no. 4, pp. 700–707, Apr. 2017.

[8] P. Roshankumar, P. P. Rajeevan, K. Mathew, K. Gopakumar, J. I. Leon, and L. G. Franquelo, "A five-level inverter topology with single-DC supply by cascading a flying capacitor inverter and an H-bridge," *IEEE Trans. Power Electron.*, vol. 27, no. 8, pp. 3505–3512, Aug. 2012.

[9] P. R. Kumar, R. S. Kaarthik, K. Gopakumar, J. I. Leon, and L. G. Franquelo, "Seventeen-level inverter formed by cascading flying capacitor and floating capacitor H-bridges," *IEEE Trans. Power Electron.*, vol. 30, no. 7, pp. 3471–3478, Jul. 2015, doi: 10.1109/TPEL.2014.2342882.

[10] K. N. Raju, M. V. G. Rao, and M. Ramamoorthy, "Hybrid modulation technique for neutral point clamped inverter to eliminate neutral point shift with minimum switching loss," in *Proc. TENCON IEEE Region Conf.*, Nov. 2015, pp. 1–5, doi: 10.1109/TENCON.2015.7373101.

[11] P. Bhatnagar, A. K. Singh, K. K. Gupta, and Y. P. Siwakoti, "A switched-capacitors-based 13-level inverter," *IEEE Trans. Power Electron.*, vol. 37, no. 1, pp. 644–658, Jan. 2022, doi: 10.1109/TPEL.2021.3098827.

[12] S. S. Lee, "Single-stage switched-capacitor module (S3CM) topology for cascaded multilevel inverter," *IEEE Trans. Power Electron.*, vol. 33, no. 10, pp. 8204–8207, Oct. 2018, doi: 10.1109/TPEL.2018.2805685.

[13] S. Mariethoz, "Systematic design of high-performance hybrid cascaded multilevel inverters with active voltage balance and minimum switching losses," *IEEE Trans. Power Electron.*, vol. 28, no. 7, pp. 3100–3113, Jul. 2013.

[14] R. A. Khan, S. A. Farooqui, M. I. Sarwar, S. Ahmad, M. Tariq, A. Sarwar, M. Zaid, S. Ahmad, and A. Shah Noor Mohamed, "Archimedes optimization algorithm based selective harmonic elimination in a cascaded H-bridge multilevel inverter," *Sustainability*, vol. 14, no. 1, p. 310, Dec. 2021.

[15] D. A. B. Zambra, C. Rech, and J. R. Pinheiro, "Comparison of neutral-point-clamped, symmetrical, and hybrid asymmetrical multilevel inverters," *IEEE Trans. Ind. Electron.*, vol. 57, no. 7, pp. 2297–2306, Jul. 2010.

[16] M. Saeedian, J. Adabi, and S. M. Hosseini, "Cascaded multilevel inverter based on DC sources with reduced number of components," *IET Power Electron.*, vol. 10, no. 12, pp. 1468–1478, Oct. 2017.

[17] H. Samsami, A. Taheri, and R. Samanbakhsh, "New bidirectional multilevel inverter topology with staircase cascading for symmetric and asymmetric structures," *IET Power Electron.*, vol. 10, no. 11, pp. 1315–1323, Sep. 2017.

[18] S. S. Lee, M. Sidorov, C. S. Lim, N. R. N. Idris, and Y. E. Heng, "Hybrid cascaded multilevel inverter (HCMLI) with improved symmetrical 4-level submodule," *IEEE Trans. Power Electron.*, vol. 33, no. 2, pp. 932–935, Feb. 2018.

[19] M. FarhadiKangarlu and E. Babaei, "Cross-switched multilevel inverter: An innovative topology," *IET Power Electron.*, vol. 6, no. 4, pp. 642–651, Apr. 2013.

[20] A. Mokhberdoran and A. Ajami, "Symmetric and asymmetric design and implementation of new cascaded multilevel inverter topology," *IEEE Trans. Power. Electron.*, vol. 29, no. 12, pp. 6712–6724, Dec. 2014.

[21] S. P. Gautam, S. Pattnaik, S. Gupta, and V. Singh, "New topology with reduced number of switches in asymmetrical cascaded multilevel inverter," in *Proc. 5th Int. Conf. Adv. Recent Technol. Commun. Comput. (ARTCom)*, 2013, Art. no. 336344.

[22] K. A. Lodi, A. Azeem, A. Sarwar, and M. Tariq, "A novel constraint-based genetic algorithm solution for SHE technique in modified PUC-5 inverter," *IEEJ Trans. Electr. Electron. Eng.*, vol. 15, no. 1, pp. 159–160, Jan. 2020.

[23] C. D. Townsend, T. J. Summers, and R. E. Betz, "Phase-shifted carrier modulation techniques for cascaded H-bridge multilevel converters," *IEEE Trans. Ind. Electron.*, vol. 62, no. 11, pp. 6684–6696, Nov. 2015.

[24] I. B. F. Citarsa, I. N. W. Satiawan, and Supriono, "A new modulation technique for a three-cell single-phase CHB inverter with un-equal DC-link voltage for improving output voltage quality," in *Proc. 2nd Int. Conf. Appl. Electromagn. Technol. (AEMT)*, Apr. 2018, pp. 73–78, doi: 10.1109/AEMT.2018.8572358.

[25] L. Wang, Q. Wu, and W. Tang, "Energy balance control of a cascaded multilevel inverter for standalone solar photovoltaic applications," *Energies*, vol. 10, no. 11, p. 1805, Nov. 2017.

[26] M. Ye, W. Ren, L. Chen, Q. Wei, G. Song, and S. Li, "Research on power-balance control strategy of CHB multilevel inverter based on TPWM," *IEEE Access*, vol. 7, pp. 157226–157240, 2019, doi: 10.1109/ACCESS.2019.2950064.

[27] M. R. Islam, A. M. Mahfuz-Ur-Rahman, M. M. Islam, Y. G. Guo, and J. G. Zhu, "Modular medium-voltage grid-connected converter with improved switching techniques for solar photovoltaic systems," *IEEE Trans. Ind. Electron.*, vol. 64, no. 11, pp. 8887–8896, Nov. 2017, doi: 10.1109/TIE.2017.2652402.

[28] M. R. Chowdhury, M. A. Rahman, M. R. Islam, and A. M. Mahfuz-Ur-Rahman, "A new modulation technique to improve the power loss division performance of the multilevel inverters," *IEEE Trans. Ind. Electron.*, vol. 68, no. 8, pp. 6828–6839, Aug. 2021, doi: 10.1109/TIE.2020.3001846.

[29] M. A. Rahman, M. R. Islam, K. M. Muttaqi, Y. Guo, J. Zhu, D. Sutanto, and G. Lei, "A modified carrier-based advanced modulation technique for improved switching performance of magnetic-linked medium-voltage converters," *IEEE Trans. Ind. Appl.*, vol. 55, no. 2, pp. 2088–2098, Mar. 2019, doi: 10.1109/TIA.2018.2881104.

[30] S. P. Biswas, M. S. Anower, M. R. I. Sheikh, M. R. Islam, M. A. Rahman, M. A. P. Mahmud, and A. Z. Kouzani, "A modified reference saturated third harmonic injected equal loading PWM for VSC-based renewable energy systems," *IEEE Trans. Appl. Supercond.*, vol. 31, no. 8, pp. 1–5, Nov. 2021, doi: 10.1109/TASC.2021.3096484.

[31] Z. Tang, M. Su, Y. Sun, B. Cheng, Y. Yang, F. Blaabjerg, and L. Wang, "Hybrid UP-PWM scheme for HERIC inverter to improve power quality and efficiency," *IEEE Trans. Power Electron.*, vol. 34, no. 5, pp. 4292–4303, May 2019.

[32] R. Shen and H. S.-H. Chung, "Mitigation of ground leakage current of single-phase PV inverter using hybrid PWM with soft voltage transition and nonlinear output inductor," *IEEE Trans. Power Electron.*, vol. 36, no. 3, pp. 2932–2946, Mar. 2021.

[33] P. Hu and D. Jiang, "A level-increased nearest level modulation method for modular multilevel converters," *IEEE Trans. Power Electron.*, vol. 30, no. 4, pp. 1836–1842, Apr. 2015.

[34] J. B. Soomro, F. Akhter, S. Ali, S. S. H. Bukhari, I. Sami, and J.-S. Ro, "Modified nearest level modulation for full-bridge based HVDC MMC in real-time hardware-in-loop setup," *IEEE Access*, vol. 9, pp. 114998–115005, 2021, doi: 10.1109/ACCESS.2021.3105690.

[35] M. H. Nguyen and S. Kwak, "Nearest-level control method with improved output quality for modular multilevel converters," *IEEE Access*, vol. 8, pp. 110237–110250, 2020.

[36] S. A. Khan, D. Upadhyay, M. Ali, M. Tariq, A. Sarwar, R. K. Chakrabortty, M. J. Ryan, B. Alamri, and A. Alahmadi, "M-type and CD-type carrier based PWM methods and bat algorithm-based SHE and SHM for compact nine-level switched capacitor inverter," *IEEE Access*, vol. 9, pp. 87731–87748, 2021, doi: 10.1109/ACCESS.2021.3087825.

[37] R. Kumar, M. S. Bhaskar, U. Subramaniam, D. Almakhles, S. Padmanaban, and J. Bo-Holm Nielsen, "An improved harmonics mitigation scheme for a modular multilevel converter," in *IEEE Access*, vol. 7, pp. 147244–147255, 2019, doi: 10.1109/ACCESS.2019.2946617.

[38] Z. Sarwer, A. Sarwar, M. Zaid, M. R. Hussan, M. Tariq, B. Alamri, and A. Alahmadi, "Implementation of a novel variable structure nearest level modulation on cascaded H-bridge multilevel inverter," *IEEE Access*, vol. 9, pp. 133974–133988, 2021, doi: 10.1109/ACCESS.2021.3113704.

[39] D. Upadhyay, S. A. Khan, M. Ali, M. Tariq, A. Sarwar, R. K. Chakrabortty, and M. J. Ryan, "Experimental validation of Metaheuristic and conventional modulation, and hysteresis control of the dual boost nine-level inverter," *Electronics*, vol. 10, no. 2, p. 207, Jan. 2021.

[40] A. Iqbal, M. Meraj, M. Tariq, K. A. Lodi, A. I. Maswood, and S. Rahman, "Experimental investigation and comparative evaluation of standard level shifted multi-carrier modulation schemes with a constraint GA based SHE techniques for a seven-level PUC inverter," *IEEE Access*, vol. 7, pp. 100605–100617, 2019, doi: 10.1109/ACCESS.2019.2928693.

[41] S. Ziaeinejad and A. Mehrizi-Sani, "PWM a-CHB converter based on trinary multilevel converter: Topology, switching algorithm, and stability analysis," *IEEE Trans. Ind. Electron.*, vol. 66, no. 6, pp. 4166–4176, Jun. 2019, doi: 10.1109/TIE.2018.2863201.

[42] Z. Ye, L. Jiang, Z. Zhang, D. Yu, Z. Wang, X. Deng, and T. Fernando, "A novel DC-power control method for cascaded H-bridge multilevel inverter," *IEEE Trans. Ind. Electron.*, vol. 64, no. 9, pp. 6874–6884, Sep. 2017, doi: 10.1109/TIE.2017.2686798.

[43] Y. Yu, G. Konstantinou, C. D. Townsend, R. P. Aguilera, and V. G. Agelidis, "Delta-connected cascaded H-bridge multilevel converters for large-scale photovoltaic grid integration," *IEEE Trans. Ind. Electron.*, vol. 64, no. 11, pp. 8877–8886, Nov. 2017, doi: 10.1109/TIE.2016.2645885.

[44] K. Boora and J. Kumar, "A novel cascaded asymmetrical multilevel inverter with reduced number of switches," *IEEE Trans. Ind. Appl.*, vol. 55, no. 6, pp. 7389–7399, Nov. 2019, doi: 10.1109/TIA.2019.2933789.

MOHD TARIQ (Senior Member, IEEE) received the B.Tech. degree in electrical engineering from Aligarh Muslim University, Aligarh, the M.Tech. degree in machine drives and power electronics from the Indian Institute of Technology (IIT) Kharagpur, and the Ph.D. degree in electrical engineering from Nanyang Technological University (NTU), Singapore, with a focus on power electronics and control.

Before joining his Ph.D. degree, he has worked as a Scientist with the National Institute of Ocean Technology, Chennai, under the Ministry of Earth Sciences, Government of India, where he has worked on the design and development of BLDC motors for the underwater remotely operated vehicle application. He is currently working as a Faculty/Postdoctoral Associate with Florida International University. He is also associated with the Energy, Power, Sustainability, and Intelligence (EPSi) Group and working on high-penetration renewable systems, grid resiliency, large-scale data analysis, artificial intelligence, electric vehicle, and cybersecurity, and an Assistant Professor at the Maulana Azad National Institute of Technology (MANIT), Bhopal, India. He is an Assistant Professor (on-leave) with Aligarh Muslim University (AMU), where he was directing various international and national sponsored research projects and led a team of multiple researchers in the domain of power converters, energy storage devices, and their optimal control for electrified transportation and renewable energy application. Previously, he has worked as a Researcher at the Rolls-Royce@NTU Corporate Laboratory, Singapore, where he has worked on the design and development of power converters for more electric aircraft. He has secured several funding's worth approximately INR 18 million for AMU. He has authored more than 225 research papers in international journals/conferences, including many articles in IEEE TRANSACTIONS/journals. He is also an inventor of more than 25 patents granted/published by the patent offices of USA, Australia, U.K., Europe, India, and China.

Dr. Tariq was a recipient of the 2019 Premium Award for Best Paper in *IET Electrical Systems in Transportation* journal for his work on more electric aircraft and the Best Paper Award from the IEEE Industry Applications Society's (IAS), the Industrial Electronic Society (IES), and the Malaysia Section-Annual Symposium (ISCAIE-2016), held in Penang, Malaysia, and many other best paper awards in different international conferences. He is also the Young Scientist Scheme Awardee supported by the Department of Science and Technology, Government of India, in 2019; the Young Engineer Awardee by the Institution of Engineers, India, in 2020; and the Young Researchers Awardee by the Innovation Council, AMU, in 2021. He is the Founder Chair of the IEEE AMU Student Branch and IEEE SIGHT AMU. He is an Associate Editor of IEEE ACCESS journal and an Editorial Board Member of *Scientific Report Nature journal*.

DEEPAK UPADHYAY received the B.Tech. degree from the University of Pune, Pune, India, and the master's degree in power system and drives from Aligarh Muslim University (AMU), Aligarh, India.

He has published research papers in various journals and international conferences. His research interests include integration of photovoltaic distributed systems, control of multilevel converters, and electric vehicles. He received the Best Paper Award from ICRP-2020.

SHAHBAZ AHMAD KHAN received the Diploma degree in engineering, the B.E. degree in electrical engineering, and the master's degree in electrical engineering (power systems and drives) from the Zakir Husain College of Engineering and Technology (ZHCET), Aligarh Muslim University.

He has coauthored various research papers in international journals and international conferences. His research interests include multilevel power electronics converter, electric vehicles, grid integration of distributed energy systems, and battery storage systems.

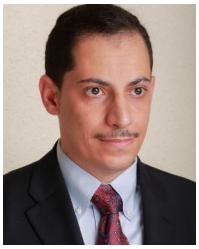

WALEED ALHOSAINI (Member, IEEE) was born in Dumat Al-Jandal, Saudi Arabia. He received the B.S. degree in electrical engineering from Jouf University, Sakaka, Saudi Arabia, in 2011, and the M.S. and Ph.D. degrees in electrical engineering from the University of Arkansas, Fayetteville, AR, USA, in 2015 and 2020, respectively. He is currently an Assistant Professor with the Department of Electrical Engineering, Jouf University. Currently, he serves as the Vice Dean of the Deanship of Scientific Research for Technical Affairs at Jouf University since August 2021 till present. He is also the Director of the Engineering and Applied Sciences Research Unit since January 2021 until present. His current research interests include renewable energy systems, model predictive control, multilevel converters, and grid-connected/stand-alone systems. He is a member of the Eta Kappa Nu.

PASI PELTONIEMI (Member, IEEE) received the M.Sc. and D.Sc. degrees in electrical engineering from the Lappeenranta–Lahti University of Technology (LUT), Lappeenranta, Finland, in 2005 and 2010, respectively. From 2010 to 2014, he was a Postdoctoral Researcher at the Laboratory of Control Engineering and Digital Systems, LUT. He became an Associate Professor in 2015. He started as an Associate Professor (tenure track) in power electronics with the Laboratory of Electrical Drives Technology, LUT University, in 2019. Currently, he is the Head of the Laboratory of Electrical Drives Technology. His research interests include electrical drives, grid-connected converters, distributed generation, P2X systems, and dc grids.

ADIL SARWAR (Senior Member, IEEE) received the B.Tech., M.Tech., and Ph.D. degrees from Aligarh Muslim University (AMU), Aligarh, India, in 2006, 2008, and 2012, respectively. From 2012 to 2015, he was with the Department of Electrical Engineering, Galgotia College of Engineering and Technology, Greater Noida, India, from 2012 to 2015. He is currently working with the Department of Electrical Engineering, AMU, since 2015. He is also working on world-bank sponsored research projects. He has published more than 50 research papers in international journals and conferences. He is a Life Member of the Systems Society of India. He has contributed a chapter in *Handbook of Power Electronics* (fourth edition) edited by M. H. Rashid.